the ground plane metallization, with the edge additionally soldered to the fixture end wall). Note the presence of the spikes predicted by theory. The frequency points at which $|S_{11}| = -10$ dB *define* a spike width and correspond to $\delta_{\text{TOTAL}} = 0.316$. (Other convenient values may be chosen as desired.) Returning to the model, δ_{2L} can be varied until the theoretical $\delta_{\text{TOTAL}} = 0.316$ spike width equals the experimental -10 dB width. Our experimental spike width of 44.7 MHz corresponds to $\delta_{2L} \approx 0.0039$, which is an angular uncertainty of 0.22°.

This small value of uncertainty was achieved experimentally as follows. Several measurements of the 50 Ω DUT were taken using the delay of the longer offset short as a variable parameter. This is illustrated in Fig. 6. The mutually consistent delay which properly characterizes the offset short corresponds to minimum spike width.

V. Summary and Conclusions

The Glasser error analysis theory [6] has been applied to network analyzer accuracy enhancement by offset shorts. The effects of DUT dependence were discussed and a useful calibration bandwidth determined. Data necessary to emulate the HP 8510 were derived and then used in the model to provide realistic results. Convenient techniques for optimizing experimental accuracy and for obtaining an estimate of the uncertainty in actual short, offset short calibration standards were presented. Due to the limited bandwidth properties of offset short calibration, multiple standards are necessary for wideband operation. The importance of the characterization procedures described above continues to apply in the multiple standards case.

The information provided in this paper should contribute to the efficiency of making chip-level measurements in a microstrip environment. This will assist in the design and realization of monolithic microwave integrated circuits. Much of the work is also applicable to offset short calibration in waveguide and other transmission line media.

Acknowledgment

The authors wish to acknowledge the fixture drawings received from MIT Lincoln Laboratory as well as helpful discussions with W. Piacentini, J. Lambert, C. Berglund, and A. Chu. The inputs of P. Rainville and R. Webster of RADC are also appreciated.

References

[1] S. Rehnmark, "On the calibration process of automatic network analyzer systems," *IEEE Trans. Microwave Theory Tech.*, vol. MTT-22, pp 447–458, Apr. 1974.

[2] R. F. Bauer and P. Penfield, Jr., "De-embedding and unterminating," *IEEE Trans. Microwave Theory Tech.*, vol. MTT-22, pp. 282–288, Mar 1974.

[3] D. Rytting, "Analysis of vector measurement accuracy enhancement techniques," presented at Hewlett-Packard RF and Microwave Symp., 1980.

[4] M. L. Stevens, "Characterization of power MESFETs at 21 GHz," ESD-TR-81-191, M.I.T. Lincoln Laboratory, Lexington, MA, Sept. 1981; AD A106673.

[5] C. D. Berglund, "Large-signal characterization amplifier design, and performance of K-band GaAs MESFET's," ESD-TR-81-296, M.I.T. Lincoln Laboratory, Lexington, MA, Dec. 1981; AD A110873.

[6] L. A. Glasser, "An analysis of microwave de-embedding errors," *IEEE Trans. Microwave Theory Tech.*, vol. MTT-26, pp. 379–380, May 1978.

[7] K. C. Gupta, R. Garg, and R. Chadha, *Computer-Aided Design of Microwave Circuits* Dedham, MA: Artech House, 1981.

[8] *HP 8510 Network Analyzer System Operating and Programming Manual*, Hewlett-Packard Company, Santa Rosa, CA, 1985

[9] *Introduction to Basic Measurements using the HP 8510*, Hewlett-Packard Company, Santa Rosa, CA, 1984.

[10] *HP 8510 Network Analyzer Operating and Service Manual*, vol. 1, Hewlett-Packard Company, Santa Rosa, CA, 1984.

[11] M. Kirschning and R. H. Jansen, "Accurate model for effective dielectric constant of microstrip with validity up to millimetre-wave frequencies," *Electron. Lett*, vol. 18, pp 272–173, Mar 1982.

On the Scalar Approximation in Fiber Optics

CHING-CHUAN SU, MEMBER, IEEE

***Abstract*—It is widely accepted that the scalar approximation is valid when the gradient of the permittivity distribution $\nabla\epsilon/\epsilon$ is small enough. Such a condition is rather demanding, however, since it precludes a rapidly varying permittivity distribution, which is usually the case in a practical optical fiber, due to some kind of fluctuation in a fabrication process. In this investigation, we derive the scalar approximation from the electric field integral equation. From the result it is seen that the applicability of the scalar approximation does not depend on the roughness in the permittivity distribution so long as the permittivity in the core is close to that in the cladding.**

I. Introduction

Mathematics is greatly simplified on applying the scalar approximation to the analysis of the propagation characteristics of guided modes in dielectric waveguides. Early in the development of the dielectric waveguide theory, Gordon [1] and Marcatili [2], among other investigators, applied the scalar approximation (together with other approximations) in studying the inhomogeneous slab waveguide and the rectangular waveguide, respectively. In 1969, in a study mainly on the step-index circular fiber (of which ϵ_r, the ratio between the permittivity in the core and that in the cladding, is close to unity), Snyder [3] obtained the scalar characteristic equation from the rigorous vectorial one. In the simplification, those terms which are of order $\epsilon_r - 1$ or smaller can be discarded. Later, Gloge [4] obtained the same scalar characteristics equation by using a set of field components that are not self-consistent. He noted that the inconsistency in transverse field components is of order $\epsilon_r - 1$.

For treating graded-index fibers or, generally, for transversely inhomogeneous fibers, Maxwell's equations in the differential form (Section II) are employed by most researchers. Thereby, it is widely accepted that the scalar approximation is valid when *the gradient $\nabla\epsilon/\epsilon$ is small enough*, as noted in [5]–[9], where ϵ denotes the relative permittivity distribution in a transverse plane. Suppose the relative permittivity distribution ϵ can be expressed as

$$\epsilon(x, y) = \epsilon_1 + (\epsilon_2 - \epsilon_1) P(x, y) \tag{1}$$

where the maximum value of $P(x, y)$ is unity such that ϵ_2 ($> \epsilon_1$) corresponds to the maximum in $\epsilon(x, y)$, and $P(x, y) = 0$ in the cladding. Having the gradient $\nabla\epsilon/\epsilon$ small enough requires that *the permittivity difference Δ be small enough and that the profile $P(x, y)$ be smooth over the fiber's cross section*, where $\Delta = \epsilon_r - 1$ and $\epsilon_r = \epsilon_2/\epsilon_1$. In other words, the scalar approximation could deteriorate if the profile $P(x, y)$ is rapidly varying (such as at a step discontinuity), even when the permittivity ratio ϵ_r becomes close to unity.

A less demanding condition on the scalar approximation can be provided by the formula proposed by Snyder *et al.* [10, eq.

Manuscript received August 18, 1987; revised January 4, 1988.

The author is with the Department of Electrical Engineering, National Tsinghua University, Hsinchu, Taiwan

IEEE Log Number 8820444.

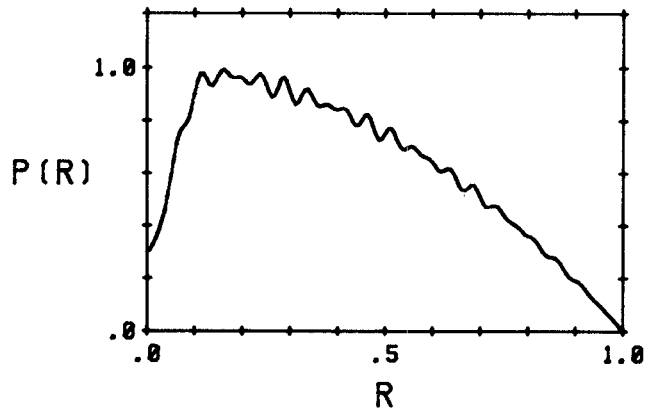

Fig 1. Fluctuations in the permittivity distribution (in a radial direction) of an optical fiber. The radial distance R is a normalized quantity.

(17)], [11, eq. (32-22)]. Such a formula relates the exact vectorial and the approximated scalar propagation constants via a quotient of two integrals. From the formula, it is seen that the error in the scalar propagation constant is of order Δ if the value of an integral involving the gradient $\nabla\epsilon/\epsilon$ is of the same order. This therefore accounts for the validity of applying the scalar approximation to circular fibers of step-index profile and some smooth profiles except a single step discontinuity [9] of order Δ. This is because, as noted in [10, note 12], an integration of the derivative of a discontinuity of order Δ results in a value of order Δ.

A profile with a single or a limited number of discontinuities of order Δ (in a radial direction) does not pose the most serious trouble in the scalar approximation. In a practical single-mode fiber, in order to make the fiber's radius larger than the wavelength of an exciting light source, the ratio ϵ_r is usually chosen close to unity, whereas owing to certain kinds of fluctuation in the fabrication process (for an example, see [12, p. 302]), the profile P may be quite rough. A representation of the roughness in the profile P is given by Fig. 1; for practical examples, we refer the reader to [12, figs. 4.3.5 and 4.5.3] and [13, figs. 106 and 107]. In view of the roughness, the question is now whether *the scalar approximation can be applied to a practical single-mode fiber where the profile P fluctuates significantly*. In Section III, we present an alternative derivation of the scalar approximation based on Maxwell's equations in the integral form, from which we will answer the question just raised.

II. The Scalar Approximation from the Differential Equation

Consider an axially uniform dielectric cylinder embedded in an infinite homogeneous medium with permittivity $\epsilon_0\epsilon_1$. For such a transversely inhomogeneous fiber, the dependences of the fields on the time and the axial coordinate (z) can be assumed to be $\exp(j\omega t - j\beta z)$. From Maxwell's equations in the differential form, one has

$$\nabla_t^2 \boldsymbol{E}_t(x,y) + \left[k_0^2\epsilon(x,y) - \beta^2\right]\boldsymbol{E}_t(x,y) + \Delta\nabla_t\left[\frac{\nabla_t P(x,y)\cdot\boldsymbol{E}_t(x,y)}{1+\Delta P(x,y)}\right] = 0 \quad (2)$$

where, $\boldsymbol{E}_t(x,y) = \hat{x}E_x(x,y) + \hat{y}E_y(x,y)$, ∇_t^2 denotes the two-dimensional Laplacian operator, $\nabla_t = \hat{x}\partial/\partial x + \hat{y}\partial/\partial y$, and $k_0^2 = \omega^2\mu_0\epsilon_0$. The last term on the left-hand side of (2) represents the effect of the polarization charge.

In those regions where the profile P is smooth, the polarization effect decreases linearly with the difference Δ. In this way, (2) becomes

$$\nabla_t^2\psi(x,y) + \left[k_0^2\epsilon(x,y) - \beta^2\right]\psi(x,y) = 0 \quad (3)$$

by discarding those terms of order Δ or smaller, where ψ denotes E_x or E_y. Along a contour of discontinuity in the profile P, one can resort to the boundary conditions. From the continuity requirement of the normal component of $\epsilon\boldsymbol{E}$, one has that the field ψ has a discontinuity at most of order Δ at a permittivity discontinuity of order Δ. And from the continuity requirements of the axial fields E_z and H_z, which can be expressed in terms of $\boldsymbol{E}_t$, we conclude that $\nabla_t\psi$ has a discontinuity at most of order Δ between the two sides of a contour of permittivity discontinuity (but not at the discontinuity). Then, by discarding those terms of order Δ or smaller, we have the boundary conditions in the scalar formulation: both ψ and $\nabla_t\psi$ are continuous in the vicinity of the permittivity discontinuity. Conventionally, these boundary conditions are stated in a loose way: both ψ and $\nabla_t\psi$ are continuous *at* a permittivity discontinuity. Practically speaking, these two sets of boundary conditions lead to the same results, however.

The question that remains is: when the profile P is rapidly varying over parts or the entirety of the fiber's cross section, is the scalar approximation still valid? Obviously, from the viewpoint of the differential equation (2), the answer is negative in general, since the magnitude of the derivatives of the profile P may be comparable to or larger than the factor $1/\Delta$.

III. The Scalar Approximation from the Integral Equation

From the magnetic vector potential $\boldsymbol{A}$ and the electric scalar potential ϕ, the electric fields can be found from the relation $\boldsymbol{E} = -j\omega\boldsymbol{A} - \nabla\phi$. Noting that current density in $\boldsymbol{A}$ is $j\omega\epsilon_0[\epsilon(x',y') - \epsilon_1]\boldsymbol{E}(x',y')$ and using the continuity equation for the charge density in ϕ, the relation becomes the electric field integral equation

$$\boldsymbol{E}(x,y) = k_0^2\int\int G(\gamma\rho)\left[\epsilon(x',y') - \epsilon_1\right]\boldsymbol{E}(x',y')\,dx'dy' + (\nabla_t - j\beta\hat{z})\int\int\frac{G(\gamma\rho)}{\epsilon_1}\left\{(\nabla_t' - j\beta\hat{z})\cdot\left[\epsilon(x',y') - \epsilon_1\right]\boldsymbol{E}(x',y')\right\}dx'dy'. \quad (4)$$

Here and throughout this investigation the integral is taken over the fiber's cross section. In (4), G denotes the two-dimensional Green's function, and it is known that

$$G(\gamma\rho) = K_0(\gamma\rho)/2\pi \quad (5)$$

where K_0 denotes the zero-order modified Bessel function of the second kind, $\gamma^2 = \beta^2 - k_1^2$ (≥ 0), $k_1^2 = k_0^2\epsilon_1$, and $\rho = [(x-x')^2 + (y-y')^2]^{1/2}$. Writing (4) explicitly, we have

$$E_x(x,y) = \Delta\left\{k_1^2\int\int G(\gamma\rho)f_x\,dx'dy' + \frac{\partial}{\partial x}\int\int G(\gamma\rho)\left[\frac{\partial f_x}{\partial x'} + \frac{\partial f_y}{\partial y'} - j\beta f_z\right]dx'dy'\right\} \quad (6a)$$

$$E_y(x,y) = \Delta\left\{k_1^2\int\int G(\gamma\rho)f_y\,dx'dy' + \frac{\partial}{\partial y}\int\int G(\gamma\rho)\left[\frac{\partial f_x}{\partial x'} + \frac{\partial f_y}{\partial y'} - j\beta f_z\right]dx'dy'\right\} \quad (6b)$$

and

$$E_z(x,y)=\Delta\left\{-\gamma^2\int\int G(\gamma\rho)f_z\,dx'dy' - j\beta\int\int G(\gamma\rho)\left[\frac{\partial f_x}{\partial x'}+\frac{\partial f_y}{\partial y'}\right]dx'dy'\right\} \tag{6c}$$

where the functions f_t denote $P(x',y')E_t(x',y')$, $i=x$, y, or z.

In the remainder of this section, we show that the scalar approximation can be made on (6) so long as the difference Δ is kept small, regardless of the functional behavior of the profile P. To begin with, it is noted that

$$0\leqslant\gamma^2\leqslant k_1^2\Delta \tag{7}$$

since $k_1^2\leqslant\beta^2\leqslant k_0^2\epsilon_2$. The derivative of the Green's function in a transverse direction is expressed as

$$\partial G(\gamma\rho)/\partial t=-\gamma(\Delta t/\rho)K_1(\gamma\rho)/2\pi \tag{8a}$$

where $t=x$ or y, Δt denotes the difference $x-x'$ or $y-y'$, correspondingly, and K_1 denotes the first-order modified Bessel function of the second kind. It is noted that both functions K_0 and K_1 are positive and monotonically decreasing. In a practical calculation, arguments in the associated Green's function range from zero to a quantity of order 1 or 10. When $\gamma\rho\to 0$, K_0 and K_1 become singular as

$$K_0(\gamma\rho)\to-\ln(1.781\gamma\rho/2) \tag{8b}$$

and

$$K_1(\gamma\rho)\to 1/\gamma\rho \tag{8c}$$

and when $\gamma\rho\to\infty$, K_0 and K_1 are equal and become vanishing as

$$K_0(\gamma\rho),\ K_1(\gamma\rho)\to(\pi/2\gamma\rho)^{1/2}\exp(-\gamma\rho). \tag{8d}$$

For a small argument $\gamma\rho\leqslant 1$, the functional values of K_0 and K_1 follow the relations, with the symbol $\to$ in (8b) and (8c) being replaced by the inequalities $>$ and $<$, respectively. For a large argument $\gamma\rho>1$, one may use (8d) as asymptotic values of both K_0 and K_1. It is essential to note that, except for the argument being very small, the functional values of K_0 and K_1 are of the same order of magnitude. Thus, the ratio between the magnitude of Green's function G and that of $\partial G(\gamma\rho)/\partial t$ is at least of order $1/\gamma$. The functional values of both K_0 and K_1 with a large argument are much less than those with a small one, and are neglected in the following analysis (the results derived in (10) still hold if this approximation is removed, by noting the factor γ in (8a)). Then, for an arbitrary positive (or nonnegative) function f, we have

$$\begin{aligned}\int\int G(\gamma\rho)f(x',y')\,dx'dy' &> \int\int\frac{-\ln(\gamma\rho)}{2\pi}f(x',y')\,dx'dy'\\ &\simeq\langle f\rangle\int\int\frac{-\ln(\gamma\rho)}{2\pi}\,dx'dy'\\ &\simeq\langle f\rangle O(\xi^2)\end{aligned} \tag{9a}$$

and

$$\begin{aligned}&\left|\frac{\partial}{\partial t}\int\int G(\gamma\rho)f(x',y')\,dx'dy'\right|\\ &\quad=\alpha\int\int f(x',y')\frac{\gamma K_1(\gamma\rho)}{2\pi}\,dx'dy'\\ &\quad<\alpha\int\int\frac{f(x',y')}{2\pi\rho}\,dx'dy'\\ &\quad\simeq\langle f\rangle O(\alpha\xi).\end{aligned} \tag{9b}$$

Here $\xi=l$ when $\gamma l\leqslant 1$, or $\xi=1/\gamma$ when $\gamma l>1$; l denotes the linear dimension of the cross section; α denotes the resultant effect of $-\Delta t/\rho$, which is a complicated function of the observation point (x,y) (in any event, the magnitude of α is less or much less than unity, since $-1\leqslant\Delta t/\rho\leqslant 1$); O stands for the order of magnitude; and $\langle\cdot\rangle$ denotes the averaged magnitude of the associated function over an area of linear dimension ξ around the observation point (x,y).

Apparently, the relations in (9) hold for a piecewise-continuous function. Thus, for a function $f_t(x,y)$ being positive over the cross section and, possibly, containing discontinuities due to the discontinuities in the profile $P(x,y)$, we have

$$\frac{A_t}{\partial A_t/\partial t}\simeq O(\xi/\alpha) \tag{10a}$$

where

$$A_t(x,y)=\int\int G(\gamma\rho)f_t(x',y')\,dx'dy'.$$

Further, it is noted that, in general, (9) is still valid for a function $\partial f_t/\partial t$ being positive and, possibly, containing singularities due to the discontinuities in $P(x,y)$. Then,

$$\frac{B_s}{\partial B_s/\partial t}\simeq O(\xi/\alpha) \tag{10b}$$

where $s=x$ or y, and

$$B_s(x,y)=\int\int G(\gamma\rho)\frac{\partial f_s(x',y')}{\partial s'}\,dx'dy'.$$

Noting $\partial G/\partial t=-\partial G/\partial t'$ and using integration by parts, we have

$$\frac{\partial}{\partial t}A_t=B_t. \tag{10c}$$

Relations similar to (9) can be given for those functions $f(x,y)$ which cannot be either positive or negative over the entire cross section. One may divide the cross section into two subregions and let $f(x,y)=f^1(x,y)-f^2(x,y)$, such that f^1 (f^2) is positive (zero) over one subregion, and is zero (positive) over the other one. Treating the integrals involving f^1 and f^2 separately, it is seen that (10) is still valid for general cases. The three relations given in (10) play a central role in this investigation. As discussed below, (10c), together with (10a) and (10b), implies that so long as the difference Δ is kept small, the effect of the polarization charge even in a rapidly varying profile is much weaker than that of the transverse polarization current, the condition upon which the scalar approximation is valid.

Consider the case where $\langle E_x\rangle$ is much greater than or is comparable to $\langle E_y\rangle$. Assume for the moment that $\langle E_x\rangle$ is greater than $\langle E_z\rangle$ by a factor $k_1\xi/\alpha$ or larger. Then, using (10) and (7) it is found that the ratio between the orders of magnitude of the first integral on the right-hand side of (6a), the second of (6a), the first of (6c), and the second of (6c) is

$$O(k_1^2\xi^2):O(\alpha^2):O(\Delta\alpha k_1\xi):O(\alpha k_1\xi) \tag{11}$$

which is consistent with the assumption just made (noticing the ratio between the first and the last terms). Note that, as seen from (6a), the quantity $\Delta(k_1\xi)^2$ should be of the order of unity. Consequently, when the permittivity difference Δ vanishes, (6a) becomes the scalar field integral equation

$$\psi(x,y)=k_0^2\int\int G(\gamma\rho)[\epsilon(x',y')-\epsilon_1]\psi(x',y')\,dx'dy' \tag{12}$$

where ψ denotes E_x. Since the integral equation (12) is obtained by discarding those terms smaller by a factor of order $\alpha^2\Delta$, it is reasonable to expect that the relative errors in both the eigenvalue β and the eigenfunction ψ are of the same order. (Based on a perturbation theory, a proof of such relations has been given for the standard eigenvalue problem in the matrix form [14].)

In the case where $\langle E_x \rangle$ is much greater than $\langle E_y \rangle$, such as in a mode excited by an x-polarized wave, it is found from (6) that, in general, the ratio between the magnitudes of the three Cartesian components is

$$E_x : E_z : E_y \simeq 1 : O(\alpha\sqrt{\Delta}) : O(\alpha^2\Delta). \tag{13a}$$

From the relation $\nabla \times \boldsymbol{E} = -j\omega\mu_0 \boldsymbol{H}$, one can find that

$$H_y = \frac{\beta}{\omega\mu_0} E_x \{1 + O[\alpha^2\Delta]\}. \tag{13b}$$

Then, H_y satisfies (12), under the same order of inaccuracy. The arguments made above can be given for E_y by simply interchanging the subscripts x and y. In summary, (12) is valid for the transverse Cartesian components, E_x, E_y, H_x, and H_y, whereas it does not hold for the axial components E_z and H_z. On applying the operator $(\nabla_t^2 - \gamma^2)$ to both sides of (12), we obtain (3), the differential equation in the scalar form.

IV. Conclusions

From the electric field integral equation a quantitative analysis of the effect of polarization charge has been given. It is found that the error due to the scalar approximation (neglecting the polarization charge) is proportional to the difference Δ, regardless of the functional behavior of the profile P. Physically, this fact is accounted for by noting that, so long as the difference Δ is kept small, a rapidly varying permittivity distribution leads to closely clustered polarization charge (positive or negative); hence the polarization effect is weakened due to self-cancellation. We have conducted many calculations for a circular fiber (using the method in [15]), and all the results support the conclusion.

References

[1] J. P Gordon, "Optics of general guiding media," *Bell Syst. Tech J.*, vol 45, pp. 321–332, Feb. 1966.

[2] E. A. J. Marcatili, "Dielectric rectangular waveguide and directional coupler for integrated optics," *Bell Syst. Tech J.*, vol. 48, pp 2071–2102, Sept. 1969.

[3] A. W Snyder, "Asymptotic expressions for eigenfunctions and eigenvalues of a dielectric or optical waveguide," *IEEE Trans. Microwave Theory Tech.*, vol. MTT-17, pp. 1130–1138, Dec. 1969.

[4] D. Gloge, "Weakly guiding fibers," *Appl. Opt.*, vol. 10, pp. 2252–2258, Oct. 1971.

[5] W. Streifer and C N. Kurtz, "Scalar analysis of radially inhomogeneous guiding media," *J. Opt. Soc. Amer.*, vol. 57, pp. 779–786, June 1967.

[6] M. Matsuhara, "Analysis of TEM modes in dielectric waveguides, by a variational method," *J. Opt. Soc. Amer.*, vol. 63, pp. 1514–1517, Dec. 1973

[7] C. N. Kurtz, "Scalar and vector mode relations in gradient-index light guides," *J. Opt. Soc. Amer.*, vol. 65, pp. 1235–1240, Nov 1975

[8] C. Yeh and L. Casperson, "Scalar-wave approach for single-mode inhomogeneous fiber problems," *Appl. Phys. Lett*, vol. 34, pp 460–462, Apr. 1979.

[9] K. Morishita, Y. Kondoh, and N. Kumagai, "On the accuracy of scalar approximation technique in optical fiber analysis," *IEEE Trans. Microwave Theory Tech.*, vol. MTT-28, pp. 33–36, Jan 1980.

[10] A. W. Snyder and W R Young, "Modes of optical waveguides," *J. Opt Soc. Amer.*, vol. 68, pp. 297–309, Mar 1978.

[11] A. W. Snyder and J D. Love, *Optical Waveguide Theory*. London: Chapman and Hall, 1983, ch. 32

[12] D. Marcuse, *Principles of Optical Fiber Measurements*. New York: Academic Press, 1981

[13] Technical staff of CSELT, *Optical Fibre Communication* New York: McGraw-Hill, 1980, ch. 3, Part I.

[14] J. H. Wilkinson, *The Algebraic Eigenvalue Problem*. Oxford· Clarendon Press, 1965, ch. 2.

[15] C. C Su and C H. Chen, "Calculation of propagation constants and cutoff frequencies of radially inhomogeneous optical fibers," *IEEE Trans. Microwave Theory Tech.*, vol. MTT-34, pp. 328–332, Mar 1986.

Saturation of the SIS Mixer by Out-of-Band Signals

LARRY R. D'ADDARIO

***Abstract*—The tendency of SIS mixers to saturate at low input signal levels is shown to depend on the total signal voltage across the junction, including frequency components outside the band of interest. If large dynamic range is to be achieved, mixers should be designed with embedding networks that present low impedances to the junction at out-of-band frequencies.**

I. Introduction

SIS (superconductor–insulator–superconductor tunnel junction) mixers allow the construction of very sensitive receivers at millimeter wavelengths, but the dynamic range of such receivers may be limited because of mixer saturation at low input powers. This has long been recognized as a significant problem [1]–[5], and approximate formulas have been presented for the input power at which departure from linear operation begins [1], [2]. Reports of experimental mixers often include measurements of this saturation power (e.g. [4], [5]). However, nearly all of this theoretical and experimental work has considered only a monochromatic input signal. In practice, it is often necessary for the receiver to accept a broad-band noise signal, such as thermal noise at room temperature. For example, strong noise sources are often used to calibrate the gain of the receiver and to determine its noise temperature; unless it can be assured that the receiver remains linear for these signals, the calibration will be in error. We will show here that it is inaccurate to assume that the saturation noise temperature T_{sat} for broad-band signals will be such that $P_{sat} = kT_{sat}B$, where P_{sat} is the saturation power measured for monochromatic signals and B is the receiver's bandwidth. This is because the broad-band signal contains power well outside this bandwidth, and, unless special precautions are taken, an SIS mixer will begin saturating because of the out-of-band signals well before the in-band power reaches P_{sat}.

II. Approximate Argument

An argument explaining the saturation mechanism of SIS mixers was first put forward by Smith and Richards [1], and later developed into an explicit formula [2]. The idea is that the small-signal gain of the mixer is a function of its dc bias, and reaches local maxima at certain voltages (photon peaks) where the mixer is normally operated. If the output frequency (IF) is low, then the output signal voltage may be considered a perturbation of the bias voltage, so that the instantaneous gain varies over the IF cycle. As the signal voltage gets large, the average gain is reduced from the peak. The embedding impedances required for low-noise, high-gain operation of an SIS mixer are such that the largest signal voltage is likely to occur at the IF, in which case this argument gives a fair description of the saturation mecha-

Manuscript received September 15, 1987; revised December 31, 1987.

The author is with the National Radio Astronomy Observatory, 2015 Ivy Road, Charlottesville, VA 22903. The Observatory is operated by Associated Universities, Inc., under contract with the National Science Foundation

IEEE Log Number 8820445.

0018-9480/88/0600-1103$01.00 ©1988 IEEE